

Energy saving passive-dynamic gait for a one-legged hopping robot

Nicholas Cherouvim and Evangelos Papadopoulos*

Department of Mechanical Engineering, National Technical University of Athens, 15780 Athens (Greece)

(Received in Final Form: October 14, 2005. First published online: January 23, 2006)

SUMMARY

Increasing the energy autonomy of a hopping one-legged robot is studied in this paper. For a particular passive gait, of all those possible, the energy dissipated per unit length of travel is shown to be less than for any other gait. This optimal gait is identified analytically, by exploiting the commonly used SLIP model to simplify real robot dynamics. Both mechanical and electrical losses are considered. The accuracy of the optimal gait analytical prediction is evaluated by a numerical analysis of a realistic robot model. Finally, restrictions imposed on executing the optimal gait due to motor limitations are studied.

KEYWORDS: Hopping robot; SLIP model; Passive hopping.

I. INTRODUCTION

Legged robots are now an area of intense research. The limitations of wheeled vehicles are obvious, when it comes to transversing the anomalous terrain present both on our planet and others. Legged robots have the potential to handle steep inclines and negotiate obstacles. The fact that legged robots do not come into contact with all the points of the ground they transverse, as in the case of wheeled vehicles, facilitates their motion over rough terrain.

Legged robots may be categorized according to their number of legs, their stability (static, dynamic), their passive or active nature, and their type and number of actuators. Robots with one,^{1,2} two,^{3–6} four,^{1,7,8} six⁹ and eight legs and also robots combining legs and wheels have been studied.¹⁰ One-legged robots may move in three dimensions,¹ or in the plane,¹¹ as in this work. Further, a legged robot is statically or dynamically stable depending on whether it is always statically balanced, or performs a motion that is stable as a whole.

Legged robots may be active, using actuators to move, or passive.¹² In the past, hydraulic^{1,3} and pneumatic actuators¹¹ have been used. In these cases, the robot is often connected to a stationary power supply. This physical connection is a constant disturbance to the robot and restricts its range. On the other hand, electric motors have been used more recently, powered by on-board batteries.^{7,9,13} Although electric motors offer the means of autonomously driving the robot, it is imperative that the robot moves in an optimum way from

an energy consumption point of view, as powerful motors and batteries are heavy.

The analysis in this paper is based on the SLIP (Spring Loaded Inverted Pendulum) model.^{14,15} This model is often used to study legged robots and is composed of a point mass attached on a spring, free to rotate around its point of contact with the ground. A similar model was used by Dummer and Berkemeier to analyze the passive dynamics and control of a one legged robot.¹⁶ An approximate map for the SLIP has been found by Schwind and Koditchek.¹⁷ To date, little if any work has incorporated energy losses into the SLIP model. Only recently has reducing energy consumption been the subject of research.^{18,19,20}

Passive running has been studied by Raibert and Buehler.^{1,12} Energy savings of 93% are reported, using passive running.¹² It is now generally accepted that passive running leads to reduced energy consumption. However, this paper differs from previous work, pointing out that various passive gaits result in different dissipated energy, so simply using a passive gait does not guarantee the least consumed energy.

In this paper, it is analytically shown that there exists a particular passive gait, of the many possible, which leads to the least dissipated energy per unit length of travel, while considering electromechanical losses. Using a SLIP model to simplify the real robot dynamics, and making mild assumptions, the optimal gait is analytically identified. To verify the accuracy of the analytical finding on a real-world robot, a realistic robot model is simulated. Finally, the effects of a torque-limited actuator on the optimal gait are studied.

II. ROBOT DYNAMICS

The one-legged robot is a system comprised of a body and a leg. The simplified dynamics of the robot, used for the analytical study, are represented here using the SLIP physical model, shown in Fig. 1. The model is comprised of a body of point mass m , a massless leg with a rest length L and a spring in the leg of stiffness k . The leg forms an angle θ with the vertical, while the length of the leg at any moment is l .

For the analytical study, the body pitching and leg inertia are ignored, and θ is thought to be small. Also, no foot slipping is considered. To verify analytical results, simulations using a *full* model with pitching and leg inertia are employed.

The system has losses, due to viscous friction at the leg with a viscous coefficient of b . To supplement energy loss,

* Corresponding author: E-mail: egpapado@central.ntua.gr

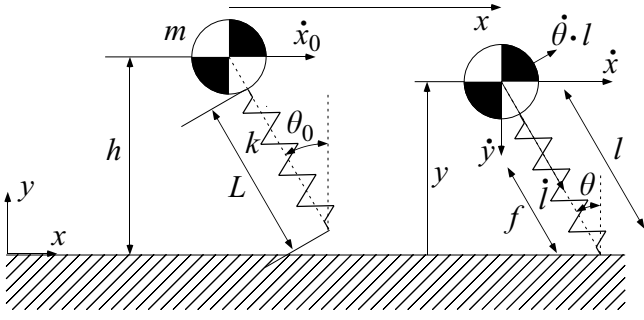


Fig. 1. The SLIP physical model at the flight apex and at a point of the stance phase.

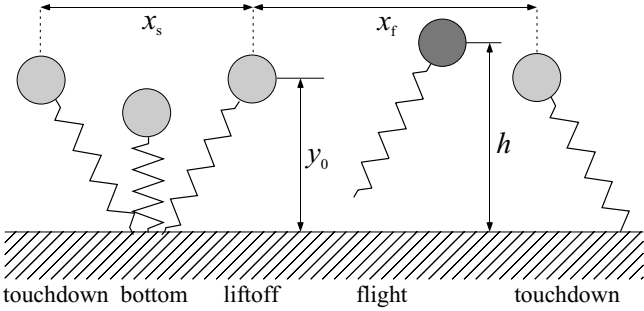


Fig. 2. Phases of the robot motion.

the robot has a motor that actuates the leg axially. The robot goes through a stance and a flight phase, see Fig. 2. During stance, the robot center of mass (CM) covers a distance of x_s , and a distance of x_f during flight, reaching an apex height h .

The equations of motion during stance may be found using a Lagrangian approach:

$$\begin{aligned} ml^2\ddot{\theta} + 2ml \cdot \dot{l} \cdot \dot{\theta} - mgl\sin\theta &= 0 \\ m\ddot{l} - ml\dot{\theta}^2 + k(l - L) + mg\cos\theta + b \cdot \dot{l} &= f \end{aligned} \quad (1)$$

where l is the leg length ($l \leq L$) and f the force the actuator exerts on the leg spring (see Fig. 1). During flight, the robot is under the influence of gravity only. Denoting the acceleration of gravity, g , and using the coordinates x, y , see Fig. 1, the equations of motion become:

$$\begin{aligned} \ddot{x} &= 0 \\ \ddot{y} &= -g \end{aligned} \quad (2)$$

III. PASSIVE RUNNING AND DISSIPATED ENERGY

If the robot has no losses, then sets of initial conditions may be found for which the robot executes a passive motion, providing the leg is swung forward during flight.¹ In this ideal case, the robot moves with zero energy consumption. However, in reality, friction does exist in the leg, so the robot will not perform more than a few hops with these initial conditions. Therefore a completely passive motion of the robot is not possible, and a motor is required for the robot to execute a sustainable gait. The motor exerts a force f on the leg that exactly compensates friction. The force f that compensates the friction force f_{fr} is:

$$f = f_{fr} = b \cdot \dot{l} \quad (3)$$

where \dot{l} is the axial leg velocity. The friction term in the equations of motion, see Eq. (1), is now canceled by the

force f . Therefore, using initial conditions that yield a passive motion for the lossless system, and a friction compensating motor, the robot will execute an active gait, very close to the passive gait. Then, the robot is studied as in the frictionless case, and the only energy required to sustain the motion is the amount dissipated due to leg friction.

It has been well shown that passive running is the most efficient type. However, depending on the initial conditions, the characteristics of a passive gait, such as the stance duration and the robot speed, will vary. Our work shows that the energy dissipated during each passive gait varies and that the differences between gaits are considerable. Hence, it is necessary to identify the gait for which the dissipated energy per meter of travel is least.

A gait is defined by a set of initial conditions, such as the initial height h of the body from the ground, the horizontal velocity \dot{x}_0 of the CM and the leg angle θ_0 at touchdown. For given values of h and θ_0 , the velocity \dot{x}_0 is uniquely defined for a 'passive' gait, in a normal working range. If the value of the apex height h is restrained, the robot may execute a wide range of 'passive' gaits with different values of the velocity \dot{x}_0 , for various values of the leg angle at touchdown θ_0 . It will be shown that for a particular value of θ_0 , the losses of the robot per unit length of travel are minimized, for a given h and \dot{x}_0 .

The mechanical power losses due to leg friction are found using Eq. (3) to be:

$$P_{fr} = b \cdot \dot{l}^2 \quad (4)$$

However, in addition to mechanical losses, electrical losses due to motor ohmic resistance exist. These do not affect the robot stability, but drain the battery and must be considered. To this end, the force f exerted on the leg by the motor is:

$$f = g_e \cdot \tau_m \quad (5)$$

where g_e is the transformation ratio of the mechanism that converts the motor revolute motion to the linear leg motion, and τ_m is the motor torque output. Neglecting mechanical losses in the motor, the torque τ_m of the motor is:

$$\tau_m = k_T i \quad (6)$$

where k_T is the motor torque constant, i the motor current. The motor ohmic losses are:

$$P_m = i^2 r \quad (7)$$

where r is the motor resistance. Using Eqs. (3), (5), (6), the ohmic power losses become:

$$P_m = b^2 \cdot r \cdot \dot{l}^2 / (g_e^2 k_T^2) \quad (8)$$

Therefore, the total power losses are:

$$P = P_m + P_{fr} = b_{tot} \dot{l}^2 \quad (9)$$

where $b_{tot} = b + b^2 r / (g_e^2 k_T^2)$.

IV. ANALYTICAL APPROACH

The optimal operating gait, from an energy consumption point of view, is analytically found. The gait is defined by the leg touchdown angle θ_0 , for a given apex height h . For the optimal gait, the quantity \hat{e} , defined as the total energy

loss during one stance, e_s , over the distance covered during one stance and one flight period, is minimized. Note that the flight energy losses are zero, as the leg is brought forward with zero torque. Therefore:

$$\hat{e} = e_s / (x_s + x_f) \quad (10)$$

For the optimum angle $\theta_{0,opt}$, for which the losses per unit length will be minimized, the derivative of \hat{e} with respect to θ_0 will be equal to zero, therefore:

$$d\hat{e}/d\theta_0 = 0 \quad (11)$$

Eq. (11) is the equation which will provide the optimum θ_0 . Below, (') denotes the derivative with respect to θ_0 . Taking Eq. (10) into account, Eq. (11) becomes:

$$\frac{e'_s(x_s + x_f) - e_s(x'_s + x'_f)}{(x_s + x_f)^2} = 0 \quad \text{or} \quad \frac{e'_s}{e_s} = \frac{x'_s + x'_f}{x_s + x_f} \quad (12)$$

Since the motor of the robot exactly compensates the friction force in the leg, the robot's movement is described by the unperturbed equations of motion:

$$\begin{aligned} ml^2\ddot{\theta} + 2ml \cdot \dot{l} \cdot \dot{\theta} - mgl\sin\theta &= 0 \\ m\ddot{l} - ml\dot{\theta}^2 + k(l - L) + mg\cos\theta &= 0 \end{aligned} \quad (13)$$

The energy lost during stance is:

$$e_s = \int_0^{T_s} P_{tot} dt = b_{tot} \int_0^{T_s} \dot{l}^2 dt = b_{tot} p \quad (14)$$

where T_s is the duration of the stance phase and:

$$p = \int_0^{T_s} \dot{l}^2 dt \quad (15)$$

Using Eqs. (14), and (15), Eq. (12) which will provide $\theta_{0,opt}$, is written as:

$$p'/p = (x'_s + x'_f)/(x_s + x_f) \quad (16)$$

Eq. (16) shows the optimum touchdown angle to be independent of leg damping. To find $\theta_{0,opt}$ from Eq. (16), the distances x_f and x_s must be functions of the touchdown angle θ_0 .

A. Expressing x_f as a function of θ_0 : The gaits considered have the same apex height h . The height of the body of the robot at liftoff, see Fig. 2, is:

$$y_0 = L\cos\theta_0 \quad (17)$$

If the liftoff angle is considered to be small, then:

$$y_0 \approx L \quad (18)$$

The flight phase duration, as the robot is under the influence of gravity only, is:

$$T_f = 2\sqrt{2h_d/g} \quad (19)$$

where h_d is the clearance at the apex point, defined as:

$$h_d = h - y_0 \geq 0 \quad (20)$$

At liftoff, the speed of the robot body in the horizontal direction is, see Fig. 1:

$$\dot{x}_{lo} = \dot{\theta}_{lo}L\cos\theta_0 - \dot{l}_{lo}\sin\theta_0 \quad (21)$$

where the subscript (*lo*) denotes a quantity at liftoff and $\dot{\theta}$ is the leg angular velocity.

It is presumed that the leg linear velocity \dot{l} does not contribute significantly to the horizontal velocity at liftoff. Mathematically, the second term of Eq. (21) is small in comparison to the first. As θ_0 is small, and $\dot{\theta}_{lo} = \dot{\theta}_0$ for a symmetric gait, Eq. (21) becomes:

$$\dot{x}_{lo} = \dot{\theta}_0L \quad (22)$$

Since the robot travels with a constant horizontal speed of \dot{x}_{lo} during flight, using the flight duration in Eq. (19), the distance x_f it covers during flight is:

$$x_f = 2L\dot{\theta}_0\sqrt{2h_d/g} \quad (23)$$

From the linearized equations of motion, it is approximately (see Appendix B):

$$\dot{\theta}_0 = -\theta_0 2\sqrt{k/(m\pi^2)} \quad (24)$$

Taking into account Eq. (24), Eq. (23), the distance x_f covered during flight is:

$$x_f = -\theta_0 4L\sqrt{2kh_d}/(\pi\sqrt{mg}) = a_1 \cdot \theta_0 \quad (25)$$

where a_1 does not depend on θ_0 .

B. Expressing x_s as a function of θ_0 : From Fig. 2, the distance covered in stance is:

$$x_s = -2L\sin\theta_0 = a_2\theta_0 \quad (26)$$

where a_2 does not depend on θ_0 .

C. Expressing p as a function of θ_0 : Using Eqs. (25) and (26), Eq. (16) gives:

$$\frac{p'}{p} = \frac{a_2 + a_1}{(a_2 + a_1)\theta_0} = \frac{1}{\theta_0} \quad (27)$$

The leg speed, derived from the linearized leg equation (see Appendix A), is:

$$\dot{l}(t) = \dot{l}_0\cos(\sqrt{k/m} \cdot t) - g\sqrt{m/k}\sin(\sqrt{k/m} \cdot t) \quad (28)$$

where \dot{l}_0 is the leg speed at touchdown. Using Eq. (28), (14b), p may be calculated as:

$$\begin{aligned} p = \frac{1}{4a_3^3} [2a_3(T_s(g^2 + a_3^2\dot{l}_0^2) - g\dot{l}_0(1 - \cos(2a_3T_s))) \\ + (-g^2 + a_3^2\dot{l}_0^2)\sin(2a_3T_s)] \end{aligned} \quad (29)$$

where $a_3 = \sqrt{k/m}$. From Eq. (28), the stance time is approximately (see Appendix A):

$$T_s \approx \pi\sqrt{m/k} \quad (30)$$

Taking into account Eq. (30), the following are true:

$$\begin{aligned}\cos(2a_3T_s) &\approx \cos(2\pi) = 1 \\ \sin(2a_3T_s) &\approx \sin(2\pi) = 0\end{aligned}\quad (31)$$

Substituting Eq. (30), (31), into Eq. (29), the integral p is given by:

$$p = \frac{1}{2}(m/k)^{3/2}(g^2 + \dot{l}_0^2 k/m) \quad (32)$$

To calculate the optimum touchdown angle $\theta_{0,opt}$ from Eq. (27), \dot{l}_0 must be a function of θ_0 .

D. Expressing \dot{l}_0 as a function of θ_0 : If \dot{y}_0 is the vertical speed of the CM at touchdown, then the duration of flight T_f is:

$$T_f = -2\dot{y}_0/g, \text{ so } \dot{y}_0 = -gT_f/2 \quad (33)$$

From Fig. 1, the vertical speed at touchdown \dot{y}_0 is:

$$\dot{y}_0 = \dot{l}_0 \cos \theta_0 - \dot{\theta}_0 L \sin \theta_0 \quad (34)$$

or, assuming again that θ_0 is small:

$$\dot{y}_0 = \dot{l}_0 - \dot{\theta}_0 L \theta_0 \quad (35)$$

From Eqs. (33) and (35) it can be found that:

$$\dot{l}_0 = a_4 \theta_0^2 + a_5 \quad (36)$$

where $a_4 = -2L\sqrt{k/m}/\pi$, $a_5 = -\sqrt{2gh_d}$.

E. Calculation of optimal touchdown angle θ_0 : Substituting Eq. (36) into Eq. (32), the quantity p becomes a function dependent only on θ_0 . Eq. (27), from which the optimum θ_0 will be determined, then takes the form of a fourth order equation:

$$n\theta_0^4 + q\theta_0^2 + w = 0 \quad (37)$$

where

$$\begin{aligned}n &= -12k^2L^2/(\pi^2m^2), \quad q = -(k/m)^{3/2}4L\sqrt{2gh_d}/\pi, \\ w &= g^2 + 2gh_dk/m.\end{aligned}$$

From Eq. (37), $\theta_{0,opt}$ is calculated:

$$\theta_{0,opt}^2 = (-q \pm d)/(2n) \quad (38)$$

where:

$$d^2 = q^2 - 4nw = \frac{160}{\pi^2}L^2\left(\frac{k}{m}\right)^3gh_d + \frac{48}{\pi^2}L^2\left(\frac{k}{m}\right)^2g^2 \quad (39)$$

In Eq. (39), the second term is smaller than the first by a factor ranging from about eight to one hundred and thirty, for the parameter values studied (see Table I). So:

$$d \cong L\sqrt{160gh_d(k/m)^{3/2}}/\pi$$

From Eq. (38), the optimum angle of touchdown $\theta_{0,opt}$ is:

$$\theta_{0,opt} = 0.96 \cdot \sqrt[4]{\frac{mgh_d}{kL^2}} \cong \sqrt[4]{\frac{mgh_d}{kL^2}} \quad (40)$$

Table I. Analytical approximation of relative errors.

Robot parameters			Optimal angle prediction error s (%)		
m (kg)	k (kN/m)	L (m)	$h_d = 0.05$ m	$h_d = 0.1$ m	$h_d = 0.2$ m
10	5	0.3	23.61	19.55	16.13
10	10	0.3	21.83	19.14	16.36
10	20	0.3	23.23	17.35	17.71
10	5	0.5	25.18	23.25	18.56
10	10	0.5	22.68	20.24	18.08
10	20	0.5	20.91	18.06	16.46
10	5	0.7	25.84	22.40	21.09
10	10	0.7	24.71	20.71	19.02
10	20	0.7	22.97	18.34	16.11

Eq. (40) provides a simple form for the optimal angle $\theta_{0,opt}$ for a given apex height h . This angle minimizes power losses and can be considered in robot design. Specifically, having chosen a desired height h , the robot parameters m , k , L , can be chosen so that $\theta_{0,opt}$ has an acceptable value, i.e. the foot does not slip and the resulting motion is not too fast.

V. NUMERICAL APPROACH

To verify the expression for $\theta_{0,opt}$ in Eq. (40), simulations were carried out in MATLAB by numerically solving the full nonlinear dynamics of the SLIP model presented in Section II. A wide range of parameters was used, specifically, for clearance, h_d , values in the range of (0.05 m, 0.2 m), for spring stiffness in the region $k = (5,000 \text{ N/m}, 20,000 \text{ N/m})$, and for the leg rest length in the region $L = (0.3 \text{ m}, 0.7 \text{ m})$. The robot body mass parameter was kept as $m = 10 \text{ kg}$. In Table I, the relative error s of the analytical formula in Eq. (40) against the numerical result, is shown, for various sets of parameters.

In Table I the error deviates little from the average value of 20.4%. Since the error is approximately constant for a wide parameter range, a corrective factor is used to increase the accuracy of Eq. (40). The factor is chosen so as to shift the average prediction error, over the above parameter range, close to zero, which occurs for a factor of 1.27. Therefore, the modified formula for the optimum touchdown angle for a given apex height is:

$$\theta_{0,opt} = 1.27 \cdot \sqrt[4]{\frac{mgh_d}{kL^2}} \quad (41)$$

The optimal angle prediction, using Eq. (41), is compared with the exact value from the simulations, for the above parameter range. In Fig. 3 the average losses of energy per unit length of travel, $\hat{\epsilon}$, as calculated in simulations, are plotted versus the touchdown angle θ_0 .

Every curve in Fig. 3 corresponds to a constant value of the clearance h_d . On each curve the touchdown angle for which $\hat{\epsilon}$ takes its minimum value is shown, as well as the touchdown angle analytically predicted to give the minimum by Eq. (41). As seen in Fig. 3, the errors are now significantly smaller and do not surpass 7% in any case.

Till now the SLIP model case was studied. To show the validity of our approach to energy saving for real robots, a

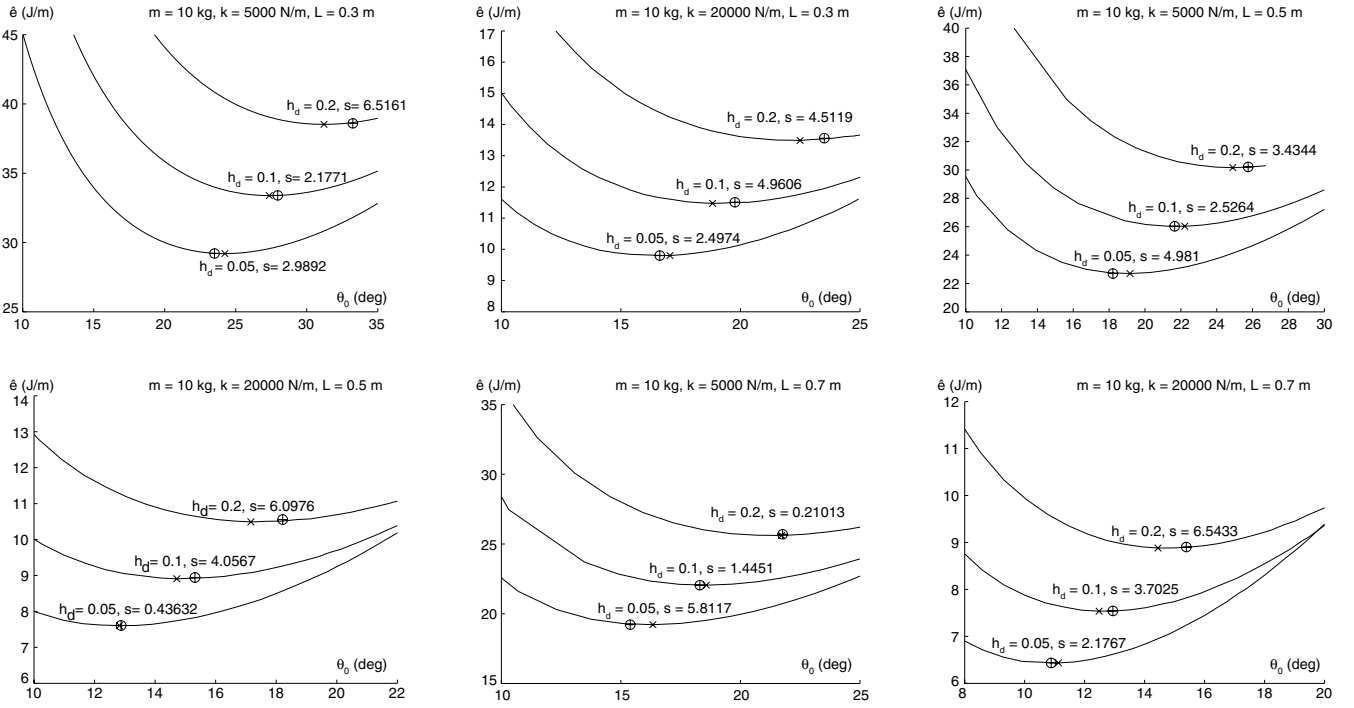


Fig. 3. Comparison of optimum point from simulation and analytical prediction. The “x” marker shows the exact minimum calculated numerically, while the “⊕” marker shows the analytical approximation of the optimal touchdown angle.

Table II. Full model parameters.

Parameter	Symbol	Value	Units
body mass	m	10	kg
body inertia	i_b	0.5	kg m ²
spring constant	k	5000	N/m
leg friction	b	25	kg/s
leg inertia	i_l	0.05	kg m ²
leg length	L	0.5	M
motor constant	k_T	0.1	Nm/A
gear ratio hip	g_{eh}	100	—
transmission ratio	g_e	30	rad/m
resistance	r	3	Ω

full realistic model is simulated, consisting of a body and leg, both with inertia, with realistic parameters. As the leg and body have inertia, a motor is used to drive the leg forward to the touchdown angle during flight. Using the full model parameters in Table II, the simulation results are shown in Fig. 4. The total energy per meter of travel is shown, as well as that used by the leg and hip motors individually.

Obviously, the optimal angle with respect to the total energy is shifted compared to the optimum angle with respect to the energy of the leg motor. However, the energy used by the hip motor is significantly smaller than the energy needed to complement leg friction losses, across the entire touchdown angle range, which explains why the optimum is not shifted far. To validate the accuracy of the full robot model simulations, the simulation software Working Model 3D was also used. In Fig. 5 snapshots are shown, together with time plots of θ , l , for the optimal angle gait at an apex height of $h = 0.57$ m, while in Fig. 6 for $h = 0.7$ m. The optimal angle is visibly larger in the second case, as predicted by Eq. (41).

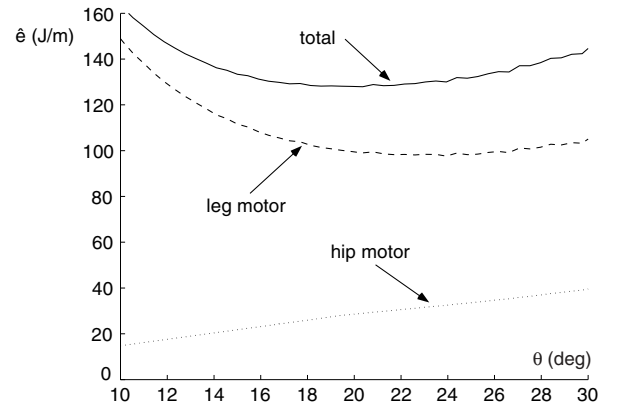


Fig. 4. Optimum working point in case of full model.

To conclude, due to the approximations made, it is expected that Eq. (41) predicts $\theta_{0,opt}$ approximately. However, it correctly predicts the qualitative effect of m , k , L and the apex height h on the optimum angle, as shown in Fig. 3, for a wide parameter range.

VI. ACTUATOR – INDUCED LIMITATIONS

The motor used on the robot is described by the following torque-speed characteristic:

$$\tau_m = (V k_m - \omega k_T^2) / r \quad (42)$$

where ω is the motor angular speed, and V is the applied motor voltage. The torque – speed characteristic is shown in Fig. 7, for the applied voltage at touchdown V_0 and for the maximum allowed V_{max} . Due to the transformation constant

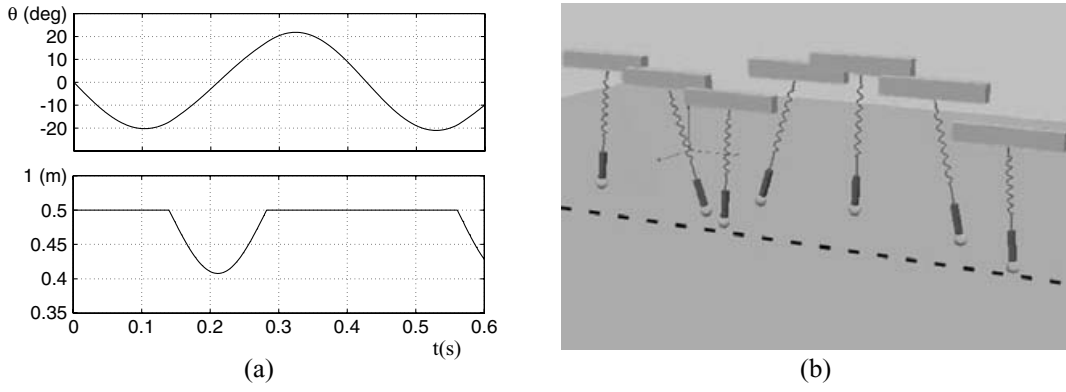


Fig. 5. Robot optimum gait, with apex height $h = 0.57$ m, (a) timeplots of θ , l , (b) Working Model 3D motion snapshots, taken every 0.1 s beginning with $t = 0$.

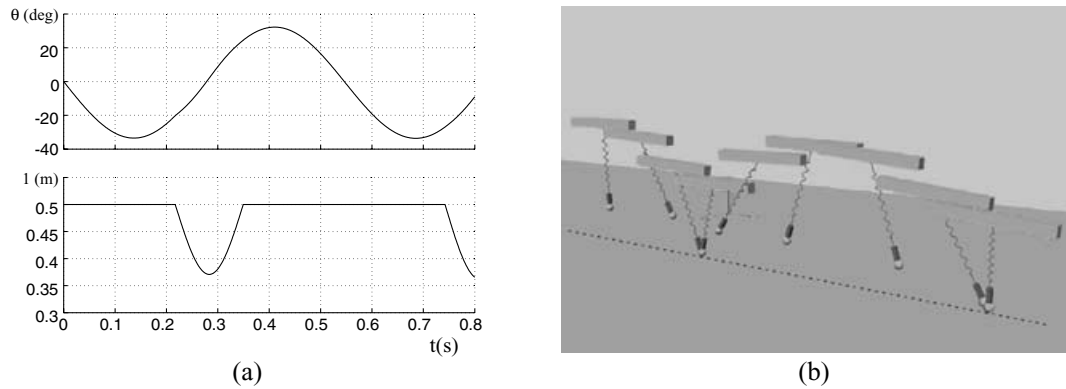


Fig. 6. Robot optimum gait, with apex height $h = 0.7$ m, (a) timeplots of θ , l , (b) Working Model 3D motion snapshots, taken every 0.1 s beginning with $t = 0$.

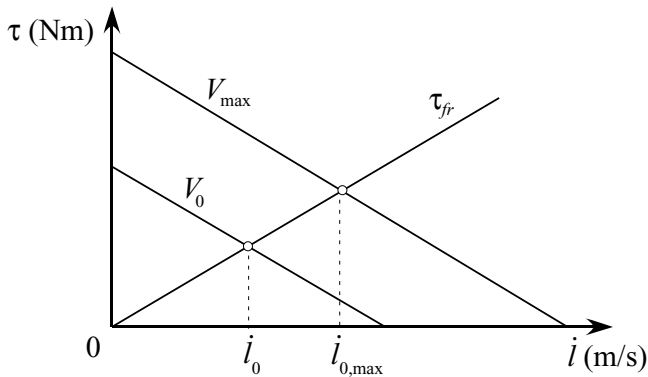


Fig. 7. Torque – speed characteristic of motor and friction compensating torque τ_{fr} .

g_e , the motor speed is:

$$\omega = g_e \dot{l} \quad (43)$$

From Eqs. (3), and (5), the required motor torque τ_{fr} to compensate friction is:

$$\tau_{fr} = b \cdot \dot{l} / g_e \quad (44)$$

and is shown in Fig. 7. Further, from Eqs. (42), and (43), the motor torque at any point is:

$$\tau_m(\dot{l}, V) = (V k_T - g_e \dot{l} \cdot k_T^2) / r \quad (45)$$

During normal operation, the motor supplies a torque given by Eq. (45), which must be equal to the torque required to compensate friction, see Eq. (44). Therefore:

$$\dot{l} = V k_T g_e / (b \cdot r + (k_T g_e)^2) \quad (46)$$

Eq. (46) expresses the relationship between the leg velocity \dot{l} and the applied motor voltage V , when friction is compensated. Since the leg velocity is greatest at touchdown, the friction force will also be greatest then, so if the motor can compensate friction at touchdown, it will be capable of compensating friction always. At touchdown, Eq. (46) gives:

$$\dot{l}_0 = V_0 k_T g_e / (b \cdot r + (k_T g_e)^2) \quad (47)$$

Eq. (47) expresses the leg velocity the robot can have at touchdown, for a touchdown voltage V_0 , so that the motor may always compensate friction. In Fig. 7 this is the leg velocity for which the friction compensating torque intersects the motor torque – speed characteristic for an applied voltage of V_0 . From Eq. (47), the greatest leg velocity the robot may have at touchdown is that which corresponds to the maximum available voltage V_{\max} :

$$\dot{l}_{0,\max} = V_{\max} k_T g_e / (b \cdot r + (k_T g_e)^2) \quad (48)$$

In Fig. 7, this is the leg velocity that corresponds to the intersection of the friction compensating torque with the torque – speed characteristic of the motor for the voltage

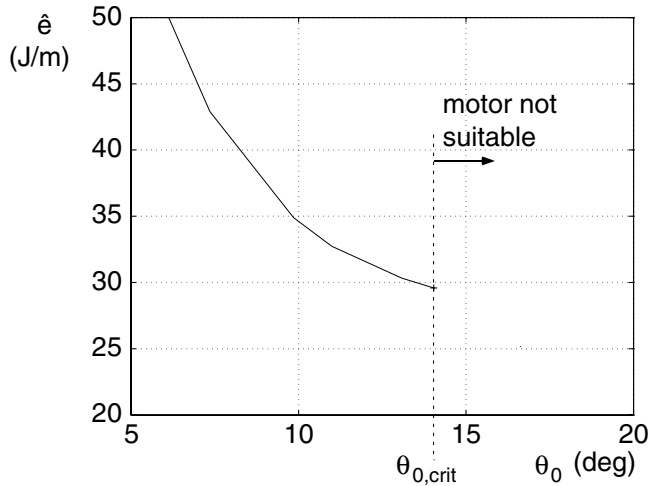


Fig. 8. Optimal θ_0 in the presence of a torque-limited motor.

V_{\max} . This means that for a gait with leg velocity \dot{l}_0 greater than the critical value $\dot{l}_{0,\max}$, the motor will be unable to supplement the friction force. Due to the symmetric stance phase condition, the critical value $\dot{l}_{0,\max}$ corresponds to a critical gait with an angle $\theta_{0,\text{crit}}$, for a given apex height h . Therefore, the leg motor is unsuitable for any gait with $\theta_0 > \theta_{0,\text{crit}}$ for the apex height h . This is because, for a given apex height h and a symmetric stance phase, a gait with a greater angle θ_0 requires a greater \dot{l}_0 , as is evident from Eq. (36).

The critical angle $\theta_{0,\text{crit}}$ may be smaller than the angle that would be optimal with an unlimited torque motor. In such cases $\theta_{0,\text{crit}}$ is the optimal θ_0 , as larger values of θ_0 are not feasible. In Fig. 8, this can be seen for a robot with $k = 10000$ N/m, $m = 10$ kg, $b = 5$ kg/s, $k_T = 0.04$ Nm/A, $g_e = 20$ rad/m, $r = 4$ Ω , $V_{\max} = 48$ V, for $h = 0.57$ m.

VII. CONDITION OF MOTOR SUITABILITY

A condition is derived that determines whether a given motor is capable of supplementing the friction force for the optimum gait predicted by Eq. (41). Eq. (36) gives the quantity \dot{l}_0 as a function of the leg angle at touchdown θ_0 , for a symmetric stance phase. For the optimum angle $\theta_{0,\text{opt}}$, \dot{l}_0 has the value given by Eq. (36):

$$\dot{l}_{0,\text{opt}} = -\sqrt{2gh_d} - 2\sqrt{k/m}L\theta_{0,\text{opt}}^2/\pi \quad (49)$$

Generally, for a motor to be capable of supplementing friction for the optimum gait, the leg velocity at touchdown, given by Eq. (49), must be smaller than the maximum leg velocity at touchdown $\dot{l}_{0,\max}$, given by Eq. (48), for which the motor can supplement the leg friction force. Because of this, and using Eqs. (41), (48) and (49), it may be found that:

$$V_{\max}k_Tg_e/(b_{\text{tot}}r + k_T^2g_e^2) \geq 2.33\sqrt{gh_d} \quad (50)$$

Eq. (50) is the condition the motor parameters must meet, for the optimum gait to be feasible, for a given clearance h_d . Note that the condition does not include the parameters k, m . This may be explained by the fact that the critical factor for the motor's ability to supplement friction is the leg velocity at touchdown. However, at touchdown the spring

is uncompressed, so the spring stiffness k does not appear. Also, Eq. (50) holds for a given apex height, for which the leg velocity at touchdown is independent of the robot mass m .

VIII. CONCLUSIONS

In this work, increasing the energy autonomy of a one-legged robot was studied. It was shown that there exists a particular passive gait, of all those possible, that leads to the least dissipated energy per meter of travel. Using the SLIP model to approximate robot dynamics, an optimal gait analytical prediction was found. Both mechanical and electrical losses were considered. The analytical prediction for the optimal gait is fairly accurate, with a simple form that correctly predicts the qualitative effect of all parameters. The accuracy of the prediction has been verified with full realistic robot model simulations. A model of a torque-limited actuator was included, to predict which gaits are possible in practice and to determine whether the optimal gait can be achieved with a given motor. Finally, a condition was derived that describes motor suitability for a given apex height and optimum gait.

Acknowledgements

Support by the State Scholarships Foundation (IKY), and the PENED 03 Program of the Hellenic Secretariat for Research and Technology is acknowledged.

References

1. M.H. Raibert, *Legged Robots That Balance* (MIT Press, Cambridge, MA, 1986).
2. W.J. Schwind and D.E. Koditchek, "Control of Forward Velocity for a Simplified Planar Hopping Robot", *Proc. of the 1995 IEEE Int. Conf. on Robotics & Automation*, Nagoya, Aichi, Japan (1995) pp. 691–696.
3. J. Hodgins, "Legged Robots on Rough Terrain: Experiments in Adjusting Step Length", *Proc. of the 1988 IEEE Int. Conf. on Robotics & Automation*, Philadelphia, Pennsylvania (April, 1988) pp. 824–825.
4. T. McGeer, "Passive dynamic walking", *Int. J. Robotics Research* **9**(2), 62–82 (April, 1990).
5. J.H. Park and K.D. Kim, "Biped Robot Walking Using Gravity-Compensated Inverted Pendulum Mode and Computed Torque Control", *Proc. IEEE Int. Conf. on Robotics & Automation*, Leuven, Belgium (1998) pp. 3528–3533.
6. S. Kajita, F. Kanehiro, K. Kaneko, K. Yokoi and H. Hirukawa, "The 3D Linear Inverted Pendulum Mode: A simple modeling for a biped walking pattern generation", *Proc. of the 2001 IEEE/RSJ Int. Conf. on Intelligent Robots and Systems*, Maui, Hawaii, USA (Oct.-Nov., 2001) pp. 239–246.
7. S. Talebi, I. Poulakakis, E. Papadopoulos and M. Buehler, "Quadruped Robot Running With a Bounding Gait", *Proc. of the Seventh Int. Symposium on Experimental Robotics (ISER'00)*, Honolulu, Hawaii (2000) pp. 281–289.
8. I. Poulakakis, E. Papadopoulos and M. Buehler, "On the Stable Passive Dynamics of Quadrupedal Running", *Proc. of the 2003 IEEE Int. Conf. on Robotics & Automation*, Taipei, Taiwan (Sept., 2003) pp. 1368–1373.
9. R. Simmons and E. Krotkov, "An Integrated Walking System for the Ambler Planetary Rover", *Proc. of the 1991 IEEE Int. Conf. on Robotics & Automation*, Sacramento, California (April, 1991) pp. 2086–2091.
10. M. Buehler, "Dynamic Locomotion with One, Four and Six-Legged Robots", *Journal of the Robotics Society of Japan* **20**(3), 15–20 (2002).

11. M. Buehler and E. Koditchek, "Analysis of a Simplified Hopping Robot", *Proc. of the 1988 IEEE Int. Conf. on Robotics & Automation*, Philadelphia, Pennsylvania (April, 1988) pp. 817–819.
12. M. Ahmadi and M. Buehler, "Stable Control of a Simulated One-Legged Running Robot with Hip and Leg Compliance", *IEEE Transactions on Robotics & Automation* **13**, No. 1, 96–104 (February, 1997).
13. D. McMordie, C. Prahacs and M. Buehler, "Towards a dynamic actuator model for a hexapod robot", *Proc. of the 2003 IEEE International Conf. on Robotics and Automation* (2003) pp. 1386–1390.
14. R.M. Ghigliazza, R. Altendorfer, P. Holmes and D.E. Koditchek, "A Simply Stabilized Running Model", *SLAM-Journal of Applied Dynamical Systems* **2**, No. 2, 187–218 (2003).
15. R.J. Full and D.E. Koditchek, "Templates and Anchors: Neuromechanical Hypotheses of Legged Locomotion on Land", *Journal of Experimental Biology* **202**, 3325–3352 (1999).
16. R. Dummer and M. Berkemeier, "Low-Energy Control of a One-Legged Robot with 2 Degrees of Freedom", *Proc. of the 2000 IEEE Int. Conf. on Robotics & Automation*, San Francisco, CA (April, 2000) pp. 2815–2821.
17. W.J. Schwind and D.E. Koditchek, "Approximating the Stance Map of a 2-DOF Monoped Runner", *Journal of Nonlinear Science* **10**, 533–568 (2000).
18. Kees van den Doel and D.K. Pai, "Performance Measures for Locomotion Robots", *Journal of Robotic Systems* **14**(2), 135–147 (1997).
19. M.F. Silva, J.A.T. Machado and A. M. Lopes, "Energy Analysis of Multi-Legged Locomotion Systems", *Proc. CLAWAR' 2001 – 4th International Symposium on Climbing and Walking Robots* (2001) pp. 143–150.
20. A. Muraro, C. Chevallereau and Y. Aoustin, "Optimal Trajectories for a Quadruped Robot with Trot, Amble and Curvet Gaits for Two Energetic Criteria", *Journal of Multibody System Dynamics* **9**, 39–62 (2003).

APPENDIX A

For small θ , the equations of motion in Eq. (13) may be linearized:

$$\begin{aligned} L\ddot{\theta} - g\theta &= 0 \\ m\ddot{l} + k(l - L) + mg &= 0 \end{aligned} \quad (\text{A1})$$

The solutions to Eqs. (A1) are:

$$\begin{aligned} \theta &= c_1 e^{a_6 t} + c_2 e^{-a_6 t} \\ l(t) &= mg \cos(\sqrt{k/m} \cdot t) / k + \dot{l}_0 \sqrt{m/k} \cdot \sin(\sqrt{k/m} \cdot t) \\ &\quad + L - mg/k \end{aligned} \quad (\text{A2})$$

where:

$$\begin{aligned} a_6 &= \sqrt{g/L} \\ c_1 &= \theta_0/2 + \dot{\theta}_0/2a_6 \\ c_2 &= \theta_0/2 - \dot{\theta}_0/2a_6 \end{aligned} \quad (\text{A3})$$

Differentiating $l(t)$ in Eq. (A2), yields:

$$\dot{l}(t) = \dot{l}_0 \cos(\sqrt{k/m} \cdot t) - g \sqrt{m/k} \sin(\sqrt{k/m} \cdot t) \quad (\text{A4})$$

Halfway during a symmetric stance phase, it is:

$$\dot{l}(T_s/2) = 0 \quad (\text{A5})$$

Solving Eq. (A5) for T_s by using Eq. (A4), yields:

$$T_s = 2\sqrt{m/k}(-\arctan(-\dot{l}_0\sqrt{k/m}/g) + \pi) \quad (\text{A6})$$

Because $k/m \gg 1\text{s}^{-2}$, the following are true:

$$\arctan(-\dot{l}_0\sqrt{k/m}/g) \cong \pi/2 \quad (\text{A7})$$

$$T_s = \pi\sqrt{m/k} \quad (\text{A8})$$

APPENDIX B

For a symmetric motion, the following is true:

$$\theta(T_s/2) = 0 \quad (\text{B1})$$

Taking into account Eq. (A2) and Eq. (B1), we have:

$$a_6\theta_0/\dot{\theta}_0 = (1 - e^{2 \cdot a_6 T_s/2}) / (1 + e^{2 \cdot a_6 T_s/2}) \quad (\text{B2})$$

Taking into account Eq. (A8), Eq. (B2) is of the form:

$$a_6\theta_0/\dot{\theta}_0 = (1 - e^{2x}) / (1 + e^{2x}) = f_1(x) \quad (\text{B3})$$

where $x = \pi\sqrt{mg/(4kL)}$. For realistic cases, the max value of x is 0.35. Plotting $f_1(x)$ and $f_2(x) = -x$ in Fig. 9, it is seen that $f_1(x) \approx f_2(x)$. Due to this, and substituting for x , it is:

$$\dot{\theta} = -\theta_0 2\sqrt{k/(m\pi^2)} \quad (\text{B4})$$

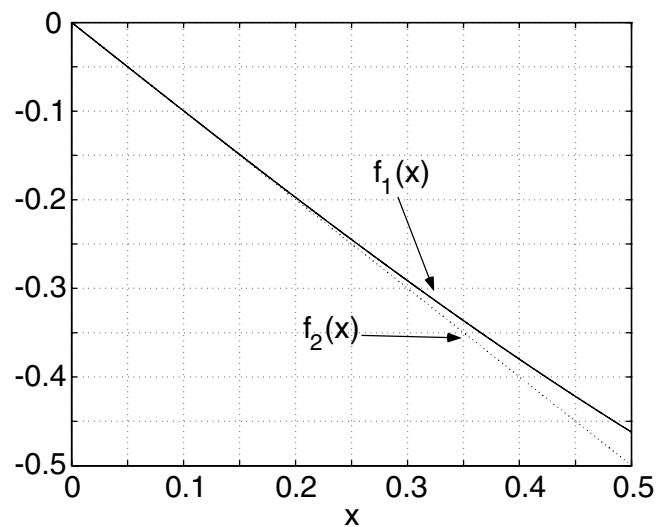


Fig. 9. Functions f_1 and f_2 .